Spectroscopic and Structural Characterization of Thermal Decomposition of γ-Mg(BH4)2: Dynamic Vacuum versus H2 Atmosphere

UNIVERSITÀ DEGLI STUDI DI TORINO

Spectroscopic and Structural Characterization of Thermal Decomposition of -Mg(BH4)2: Dynamic Vacuum Vs. H2 Atmosphere

Jenny G. Vitillo, Silvia Bordiga, Marcello Baricco

J. Phys. Chem. C, 2015, 119 (45), pp 25340–25351

DOI: 10.1021/acs.jpcc.5b06806

Spectroscopic and Structural Characterization of Thermal Decomposition of γ-$Mg(BH_4)_2$: Dynamic Vacuum Vs. H_2 Atmosphere

Jenny G. Vitillo,[†‡*] *Silvia Bordiga,*[†] *Marcello Baricco*[†]

[‡]Department of Science and High Technology, Università dell'Insubria, Via Valleggio 11, 22100 Como, Italy.

[†]Department of Chemistry, NIS Center and INSTM, University of Turin, via Quarello 15, I-10135 Torino, Italy.

ABSTRACT. $Mg(BH_4)_2$ attracts a particular interest as material for hydrogen storage because of its high gravimetric capacities and being suggested as a rehydrogenable compound. Although extensively studied, besides the whole decomposition process, a large debate is still present in the literature about the temperatures leading to the different (and in many cases, unknown) products. In this paper, an ad hoc designed thermogravimetric study, together with a critical review of literature data, allowed to identify the products for low reaction rates. Two reaction environments have been considered: dynamic vacuum and hydrogen atmosphere. In order to guarantee quasi equilibrium conditions, the samples were obtained after 10 h isotherms in the RT-400 °C range. The decomposition of γ-$Mg(BH_4)_2$ has been here characterized adopting a new approach and by XRD and medium infrared spectroscopy, together with experimental techniques used for the first time for this process (Far-IR and UV-Vis-NIR spectroscopies). Density functional calculations were performed to help the identification of the amorphous products. A possible process mechanism was delineated and in particular that: (a) $Mg(BH_4)_2$ decomposition starts at 200 °C; (b) MgB_4H_{10} is

proposed, for the first time, as the phase responsible for its reversibility for $T < 270$ °C, which would implicitly restrict the $Mg(BH_4)_2$ reversible capacity to 3.7 mass%.

Keywords: $Mg(BH_4)_2$, hydrogen storage, borohydrides, density functional calculations, IR spectra, boranes.

INTRODUCTION

Complex metal hydrides represent a particularly important class of materials for hydrogen storage because of the high gravimetric H_2 capacities reached by most of these compounds, in particular borohydrides (e.g. 18.5 mass% H_2 in $LiBH_4$). These high gravimetric capacities are possible because, at difference of classical metal hydrides where hydrogen is present as interstitial guest in the metal host lattice, in complex hydrides a covalent bond exists between the H atom and an atom of the framework, allowing to store very high quantities of hydrogen. Nevertheless, the covalent nature of the chemical bond asks for a true chemical reaction for hydrogen release, making more difficult, and in most cases impossible, the rehydrogenation of the system. Moreover, very high temperature and the release of harmful by-products as B_2H_6 are often characteristics of their decomposition. Between borohydrides, $Mg(BH_4)_2$ (14.5 mass% H_2) is the only representative able to partially rehydrogenate in mild conditions (1-2 mass% at 210-285 °C and 100-155 bar).[1-3] The total rehydrogenation from MgB_2 has been reported only at 350 °C and 800 bar, resulting in a mixture of $Mg(BH_4)_2$ and $MgB_{12}H_{12}$.[4-6] Moreover, $Mg(BH_4)_2$ is able to release up to 6 mass% in mild temperature conditions (300 °C)[1] and the gaseous product of its decomposition is hydrogen with only slight traces of diborane.[7, 8] In order to improve its reversibility, several studies have been aimed to shed light on the evolution of the phases formed during the complex dehydrogenation of this material:[1, 3, 9-11] nevertheless, its decomposition mechanism is still unclear. In fact, several open questions are under debate upon the decomposition mechanism of $Mg(BH_4)_2$ (a schematic list of them is reported in the Supporting Information). In the present paper, most of these questions have been addressed by adopting an experimental approach to the problem derived by a critical analysis

of the results reported in the literature. In fact, most of the difficulties occurring in the identification of the decomposition intermediates (Mg-B-H species, in the following) arises from the amorphous nature of the intermediates themselves and of some of the high temperature $Mg(BH_4)_2$ polymorphs.[12] A large number of possible $Mg(BH_4)_2$ structural polymorphs (crystalline or amorphous) has been experimentally determined or suggested (see Supporting Information and Figure S1 for further information). [9, 13-19] At present, seven different crystalline polymorphs have been identified for $Mg(BH_4)_2$: α ($P6_122$),[20] β (Fddd),[13] γ (Ia-3d),[14] δ_{HP} ($P4_2nm$), ζ ($P3_112$)[16] and ε.[9, 17] Among them, only α, β, ζ and γ have been structurally determined (see Figure S1),[9, 13-20] so that an assessment of thermodynamic properties has been possible.[21] Different amorphous polymorphs of $Mg(BH_4)_2$ have been reported[12, 22] in the temperature range interested by the starting of the borohydride decomposition. Some of these polymorphs undergo to a further phase transition upon quenching ($\varepsilon \rightarrow \alpha$), making difficult to compare results of this process for in situ and ex situ annealing.[9] Besides the intrinsic complexity of the decomposition process, misinterpretation are often related to inaccuracy in the experimental procedures adopted, as already pointed out by Paskevicius et al.,[9, 22] or to an incomplete analysis of the obtained results. As examples: *in situ* XRD decomposition studies performed on sealed capillaries in Ar are commonly analyzed without taking into account the increasing concentration of hydrogen in the reaction atmosphere; the sublimation of some products, especially of elemental Mg, in vacuum/inert gas flow is not taken into account in gravimetric/volumetric studies at low temperatures (<400 °C);[23] static vacuum is considered coincident with vacuum instead with hydrogen atmosphere; the results obtained ex situ can be different from the ones reachable in situ because of phases transition (melting transformation to amorphous phase, or ε transition to α after quenching at RT).[9] In the present study, some existing open points have been clarified as follow, by adopting a new approach designed after a critical review of the results reported so far: (a) thermal isothermal treatments prolonged in time (20 h), in order to reasonable consider negligible the influence on the results of the process kinetics; (b) extensive characterization of the pre-melting temperature range, rarely considered in the literature;

(c) use of several spectroscopic techniques in order to cover a wide range of energy (from UV to far infrared) coupled with density functional calculations, with the aim to determine the amorphous product responsible for the reversibility of the decomposition process for T lower that the $Mg(BH_4)_2$ melting temperature ($270 \leq T \leq 290$ °C).[9] Between the possible isomorphs of $Mg(BH_4)_2$, γ phase has been chosen in order to facilitate the comparison with one of the reference articles in the literature[9] and because this phase is receiving an increasing interest for its porous structure, characterized by a very large surface area (1160 m^2 g^{-1}).[14, 20] Moreover, for temperatures higher than 190 °C, it undergoes to a phase transformation to the β' phase making its decomposition path likely coincident with that of the most studied α phase.[9] This means that previous studies focused on the composition of α and β phases can be used here for comparison. In the first part of this study, the decomposition rate of γ-$Mg(BH_4)_2$ at different temperatures has been determined by means of a microbalance by heating the sample up to 450 °C and leaving it to isothermally equilibrate at selected intermediate temperatures for 10 h. Two different environments have been imposed: (i) dynamic vacuum ($p < 10^{-4}$ mbar); (ii) 300 mbar of H_2. This gravimetric analysis allowed to draw several interesting conclusions and in particular the slow decomposition rate in the pre-melting temperature range, not allowing to reach the equilibrium even after 10 h of annealing. Only few studies exist in the literature, reporting the characterization of materials treated isothermally for very long time,[1, 24] but all of them are focused in the post-melting temperature range. The decomposition in this temperature range, although characterized by fast rate and high H_2 release, is nevertheless accompanied by a separation of products, leading to severe conditions for rehydrogenation.[4-6] The characterization of the pre-melting temperature range is then more interesting from an applicative point of view. Although it has been reported that the environment determines different reaction products in the post-melting temperature range,[9, 24, 25] no studies exist for the pre-melting temperature one. Recently, Yan et al.[10] reported a study where $Mg(BH_4)_2$ was

decomposed under dynamic vacuum also at 265 °C for 20 h, that is at a temperature where the melting of the material can be already observed.

Because of the conclusions derived from the TGA analysis, the decomposition of γ-$Mg(BH_4)_2$ has been characterized after treatments of 20 h in dynamic vacuum and in H_2 atmosphere at increasing temperatures (25, 150, 190, 200, 205, 225, 250, 300 and 400°C). The range between 250 and 300 °C has not been considered in the present paper because of the larger dependence of the decomposition process on the thermal history of the material, making difficult the reproducibility of the results. The samples were analyzed by means of X-ray powder diffraction (XRD) and by spectroscopic techniques covering a wide spectral range going from 100 to 50000 cm^{-1}. The use of spectroscopy has been dictated by the amorphous nature of some intermediates. The infrared characterization of $Mg(BH_4)_2$ and of its decomposition products has been previously reported,[2, 3, 9, 10] but it was restricted to the medium infrared region. Such a broad frequency range was considered in order to identify the larger number of characteristic spectroscopic features of the dehydrogenation products. Being lacking in the literature the infrared spectra of all the possible intermediates, density functional (DFT) calculations have been also carried out in order to help in the individuation on the reaction intermediates in the pre-melting temperature range.

MATERIALS AND METHODS

Materials. γ-$Mg(BH_4)_2$ was purchased from Sigma Aldrich (95% purity, 54978-1G, batch #MKBK0970V). XRD analysis of the as received sample indicated the sample contains ca. 78 mol% of γ phase and 22 mol% α phase, with no other phase present (see Supporting Information for further details).[26] The materials have been handled in inert atmosphere (M Braun Lab Star Glove Box supplied with pure 5.5 grade Nitrogen, <0.5 ppm O_2, <0.5 ppm H_2O). H_2 (6.0 N purity) was used for thermal treatments. Because of the conclusions derived from the TGA analysis, the

decomposition of γ-$Mg(BH_4)_2$ has been characterized after treatments in dynamic vacuum ($p < 10^{-4}$ mbar) and in 200 mbar of H_2 atmosphere on a glass vacuum line at increasing temperatures (25, 150, 190, 200, 205, 225, 250, 300 and 400°C), leaving the sample to isothermally equilibrate at each temperature for 20 h. Before the treatment in hydrogen, the sample was degassed for 1 h at RT. As sample containers for the preparation of the samples by annealing, wide bottom glass tubes where used as suggested in previous studies,[9] in order to facilitate the visual observation of the sample and to minimize the temperature gradient in the different portion of the sample. About 150 mg of fresh powder has been used for each annealing treatment. After each isotherm, the system was cooled to room temperature, degassed for 10 minutes, and characterized within 6 hours from the end of the thermal treatment.

Powder XRD measurements. Powder X-Ray Diffraction measurements were performed in the 2θ range 2° – 90° (step size of 0.017°, time per step 200 s) using a laboratory diffractometer (Panalytical X'Pert Pro Multipurpose Diffractometer) equipped with Ni filtered Cu source in Debye-Scherrer geometry. Samples were sealed into boron silica glass capillaries of internal diameter 0.8 mm in a protected atmosphere. Diffraction patterns were refined with Rietveld method using MAUD (Material Analysis Using Diffraction) program.[27, 28]

Micrograviметric measurements. An intelligent gravimetric analyzer (IGA-002, supplied by Hiden Analytical Ltd, UK) was used, equipped with a fast heating furnace for the temperature control and an ultrahigh vacuum system (10^{-6} mbar). Before each measurement, the sample was degassed for 12 h at RT. Buoyancy effects were found to affect the weight to less than 0.25% in the pressure and temperature range considered and for that reason were neglected. The measured weights were affected by an absolute error lower than 0.01 mg in the conditions adopted (starting sample weight of about 100 mg), corresponding to an error in the calculated mass loss comprised in the range 0.03-0.08 mass%.

FTIR spectroscopy. Attenuated Total Reflection Infrared (ATR-IR) spectra (2 cm^{-1} resolution, average on 256 scans) were collected in the 4000-375 cm^{-1} range on loose powder on a Bruker Alpha spectrophotometer, equipped with an internal reflection element in diamond and placed in the glove box. Intensity of the spectra has been corrected for the effective thickness value for the different incident wavelengths. Far-IR measurements were carried out in the 600-100 cm^{-1} range on a Bruker Vertex 70 spectrophotometer, by averaging 32 scans (2 cm^{-1} resolution) on pellets obtained by diluting the powder samples in a paraffin wax (Sigma Aldrich) in a 1:6 volume ratio, by mechanical mixing in an agate mortar.

UV-Vis-NIR spectroscopy. Diffuse reflectance UV-Vis-NIR measurements were performed on a Varian Cary 5000 spectrometer equipped with a reflectance sphere on loose powders diluted in Teflon (Sigma Aldrich, previously degassed at 120 °C for 12 h) in 1:10 mass ratio. For the measurements, the samples were placed inside the standard powder cell of the instrument.

Computational methods. Calculations have been performed with the *Gaussian 09* software package.[29] All the systems under study have been optimized by means of the Becke's three-parameters hybrid exchange functional[30] supplemented with the Lee, Yang and Parr's gradient-corrected correlation functional[31] (B3-LYP). For all the elements (Mg, B and H), the fully optimized triple-ζ valence basis sets proposed by Ahlrichs *et al*.[32] with polarization (TZVp) have been adopted. Geometry optimization has been carried out by means of the Berny optimization algorithm with analytical gradient. The thresholds were set to 0.000450 and 0.000300 a.u. for the maximum and the rms forces respectively; and to 0.001800 and 0.001200 a.u. for the maximum and rms atomic displacements, respectively. A (99,590) pruned grid was used (i.e. 99 radial points and 590 angular points per radial point).

Harmonic frequencies have been obtained by analytically determining the second derivatives of the energy with respect to the Cartesian nuclear coordinates and then transforming them to mass-

weighted coordinates. No scaling factor has been adopted. The calculated spectra have been obtained by simulating the peak broadening of each signal by means of a Lorentzian curve having a full width half maximum (FWHM) of 25 cm^{-1}.

RESULTS

Microgravimetric analysis. In the first part of this study, the decomposition rate of γ-$Mg(BH_4)_2$ at different temperatures has been estimated by means of a microbalance by heating the sample up to 450 °C (1°C/min) at increasing temperatures (25, 150, 190, 205, 225, 250, 300, 350, 400 and 450 °C) and leaving it to isothermally equilibrate at each temperature for 10 h. The use of a gravimetric apparatus instead of a volumetric instrument has been dictated by the higher sensitivity of gravimetric measurements (making them particularly suitable for the study of slow kinetics decomposition processes) and to the direct dependence of the results on the weight of the species evolved. Two different environments have been imposed: (i) dynamic vacuum ($p < 10^{-4}$ mbar); (ii) 300 mbar of H_2. Several steps at temperature lower than the melting temperature of $Mg(BH_4)_2$ have been considered.[9] In fact, although it has been claimed in several studies that $Mg(BH_4)_2$ would decompose only after melting, as typical of borohydrides, in different papers it has been reported as the decomposition would start at significantly lower temperature: 100°C (Ar flow),[2] 150°C (Ar flow),[17] 205°C (dynamic vacuum)[1] or 227°C (He flow).[33] Actually, the close proximity of the melting temperature to the temperature at which the decomposition rate significantly increases, has been at the basis of the diverging opinion on the melting behavior of $Mg(BH_4)_2$, unraveled only recently (see Ref. 22 and Supporting Information for further details). The results obtained in the present thermogravimetric (TGA) study are reported in Figure 1 and in Table 1, where they are compared with gravimetric studies previously reported. From Figure 1, it is evident as the effect of annealing environments has a strong impact on the mass loss at all the temperatures (compare the orange and the black curves in Figure 1, corresponding to decomposition in vacuum and hydrogen,

respectively). Another interesting information that can be deduced from Figure 1 is that the mass loss is important also in the pre-melting temperature range ($T < 260$ °C), associated to decomposition products with high vapor pressure (e.g. smaller boranes).

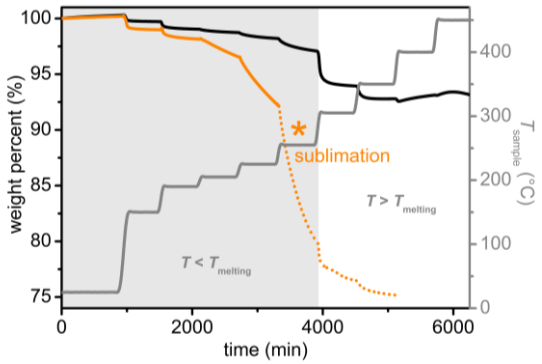

Figure 1. Thermal decomposition of γ-$Mg(BH_4)_2$ in the RT-450 °C range in dynamic vacuum ($p < 10^{-3}$ mbar, orange curve) and in hydrogen atmosphere ($p = 300$ mbar, black curve). The temperature curve is also reported as grey curve. The pre-melting temperature range is highlighted by means of a light grey area. The asterisk marks the beginning of sublimation for the decomposition in vacuum: the part of the curve affected by sublimation has been reported as a dotted line.

For $T < 260$°C, the decomposition rates are so slow to not allow reaching the equilibrium even after 10 h of annealing. On one hand, this explains the reason why it has been for long time reported that the decomposition of $Mg(BH_4)_2$ would be possible only for $T > 260$ °C. Moreover, a direct conclusion from this plot is that, for heating rate ≥ 1 °C/min, a strong overlap is expected between phases that would form in equilibrium condition at different temperatures, making difficult their identification and intrinsically making their appearance strongly dependent on the heating rate adopted.[17] The large dependence of the mass loss on the heating rate is evident by comparing the values reported in Table 1: in particular, for the measurements performed under He atmosphere (2nd, 3rd and 4th column) the only difference in the decomposition conditions is the heating rate, so that a significant increase of the mass loss is observed by lowering the velocity from 10 to 1 °C/min.

It is worth noting that, in dynamic vacuum conditions, a strong sublimation was observed starting from temperature higher than 225 °C (see asterisks and dotted part of the orange curve in Figure 1). The sublimation was visually observed by degassing the sample in a glass tubes. This aspect is

usually neglected in experiments and it is expected to hinder the rehydrogenation of the system back to $Mg(BH_4)_2$ if a too low H_2 backpressure is used. This point is expected to be particularly important for complex hydrides in general, in the sense that a lowering in the cyclability of the hydrides is expected if the decomposition is carried out in dynamic vacuum, because of the removal of the most volatile products (e.g. smaller boranes and Mg).

Table 1. Cumulative mass loss of the $Mg(BH_4)_2$ expressed as mass% at increasing temperatures in H_2, He and Ar atmospheres and in dynamic vacuum, as determined on gravimetric apparata.

***T* (°C)**	**H_2[a]**	**He[b]**	**He[c]**	**He[d]**	**Ar[e]**	**Ar[f]**	**vacuum[g]**
150	0.28					1.4	1.01
165					0.88	1.87	
190	0.95	0.0				2.25	1.85
205	1.26	0.14				2.56	3.4
212					1.31	2.63	
225	1.77	0.49				2.86	7.89
250	2.91	1.03		0.0		3.55	19.94
300	6.06	3.84	3.3			6.59	23.51
330		7.24	5.9		5.34	8.59	
350	7.21	10.24				9.67	24.81
365			11.0		9.59	10.32	
400	6.96	12.86				11.05	
450	6.65	13.51				11.7	
500				13			
527			14.4				

[a] γ-phase, 300 mbar, 10 h of equilibration at each temperature (this work). The calculated mass loss were affected by an error estimated in the range 0.03-0.08 mass%.

[b] α-phase, 2°C/min, 50 ml/min, from Ref. 8.

[c] β-phase, 5°C/min, 150 ml/min, from Ref. 33.

[d] α-phase, 10°C/min, 50 ml/min, from Ref. 7.

[e] γ-phase, 1°C/min, 100 ml/min, from Ref. 17.

[f] γ-phase, 2°C/min, 50 ml/min, from Ref. 2.

[g] γ-phase, dynamic vacuum (turbolecular-equipped system), 10 h of equilibration at each temperature (this work). The calculated mass loss were affected by an error estimated in the range 0.03-0.08 mass%.

The thermogravimetric signals in Figure 1 indicate that for the decomposition both in vacuum and in hydrogen atmosphere, gas release is observed already at 150 °C (first and last column of Table 1). This gas evolution can be related to the loss of species encapsulated in the pores (solvent and B_2H_6)[26] or to a partial dehydrogenation of the borohydride, that would start then at very low temperatures.[2, 17] This result was already reported by David et al.[17] in a coupled thermogravimetric / mass spectroscopic (TGA-MS) study in Ar flow. Nevertheless, the mass loss at this temperature was so low to prevent in that study the discrimination between the possible desorbed species by mass spectroscopy (H_2, B_2H_6, solvent). The dehydrogenation of $Mg(BH_4)_2$ can be reasonably ruled out for $T \leq 190$ °C on the basis of the observation that the decomposition of α-$Mg(BH_4)_2$ (also for slow heating rates, 2 °C/min)[8] would start only for $T > 190$ °C. γ-$Mg(BH_4)_2$ pores are occupied by solvent and B_2H_6 molecules that can be released only after activation in supercritical gas[34] or pore collapse, the latter due to chemical reaction with external reagents[26] or to phase transitions. Although the mass loss observed for $T \leq 190$ °C for γ-$Mg(BH_4)_2$ can be related to the different surface area of this isomorph that would facilitate the kinetics of decomposition, this result can be likely related to the released of the trapped species, as a consequence of the transition of γ-$Mg(BH_4)_2$ to lower surface area isomorphs. This conclusion is also supported by the results obtained by the XRD and spectroscopy characterization (see below).

An important decomposition for $190 < T < 270$ °C, that is for temperatures significantly lower than the melting temperature, is noticed for both hydrogen and vacuum atmosphere. This

observation can be visible only in a gravimetric measurements, being the kinetics so slow to hinder this observation in volumetric apparata. This result suggests that the dehydrogenation temperatures of $Mg(BH_4)_2$ reported so far should be considered as apparent being largely affected by kinetics if very long reaction time are not adopted. This would also suggest that the reported catalytic effect of some compounds on borohydrides, lowering their decomposition temperature below their melting temperature, could be in some cases related to a physical particle dispersion, but not strictly related to a chemical "activity" of the additive. This is in agreement with recent results on γ-$Mg(BH_4)_2$ where it was verified that the effect of ball milling on the kinetics of decomposition was similar with and without additives.[2] Analogously, the lowering of the $Mg(BH_4)_2$ decomposition temperature by nanodispersing it on supports may then have mainly a kinetic origin, not necessarily asking for any activation of the B-H bond by the interaction with the support.[35]

All the results reported in the following are referred only to the unsublimated fraction of the samples, whereas a characterization of the sublimated fraction has not been reported for the **vac** samples. Attempts to characterize the sublimated part have been performed but because of the small sample amounts and the likely contamination of the sublimated part by the unsublimated one in the glove box, the results obtained were so uncertain that have not been reported. Nevertheless, it is important to stress that the IR spectra recorded for the sublimated fraction did not shown any extra signals with respect to the ones measured for the unsublimated part.

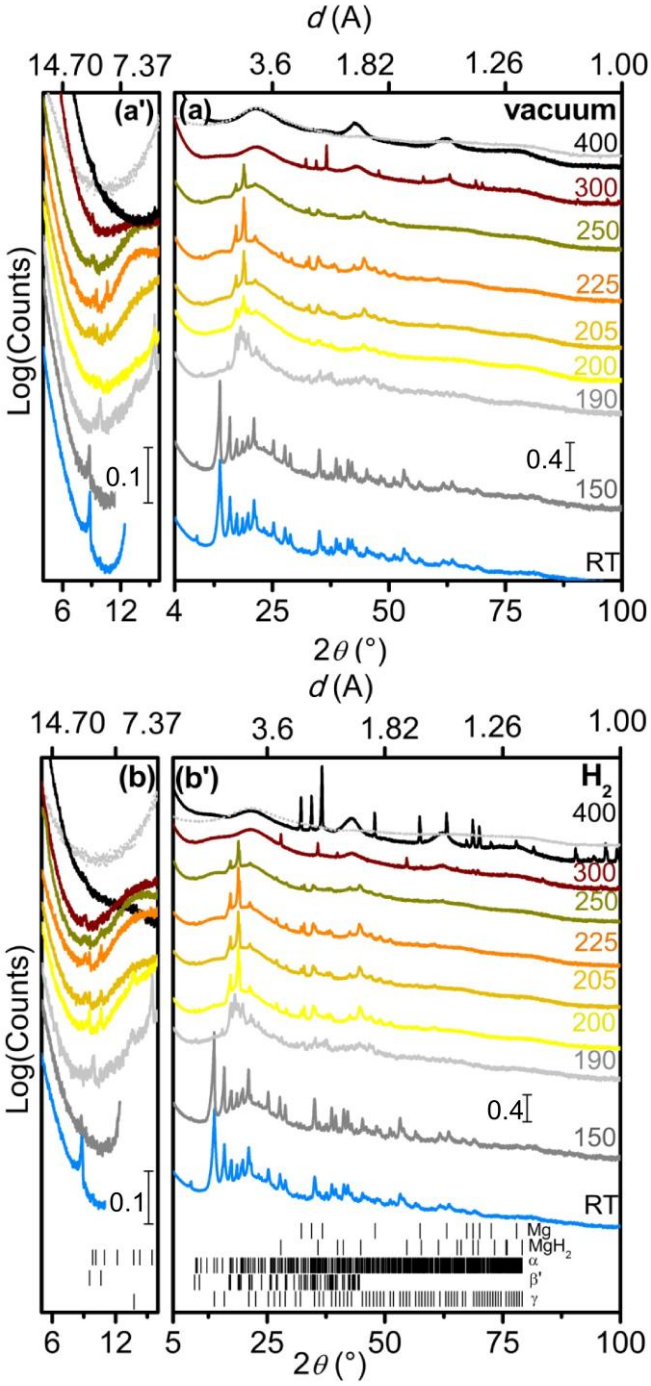

Figure 2. XRD patterns recorded after thermal decomposition of γ-$Mg(BH_4)_2$ in the RT-400 °C range in (a) dynamic vacuum ($p < 10^{-3}$ mbar) and (b) in hydrogen atmosphere (p = 300 mbar). (a') and (b'): inset in the 4-16° range. The pattern of an empty borosilicate capillary of 0.8 mm in diameter is also shown for comparison (dotted light grey line). The color legend referring to the treatment temperature (in Celsius) is reported in the graph.

X-Ray Powder Diffraction. XRD patterns of γ-$Mg(BH_4)_2$ after treatment for 20 h at increasing temperatures in dynamic vacuum (**vac**) and in H_2 atmosphere (**H2**) are reported in Figure 2 (top and

bottom, respectively). The pattern obtained on the empty capillary is reported for comparison (dotted light grey line) and it was characterized by a broad halo at about 22°. The description of the pattern evolution up to 250 °C is basically the same for the **vac** and the **H2** samples, although the differences observed in the mass loss in the two conditions (see Figure 1). For what concerns the pattern evolution with temperature, (i) at RT the sample shows the presence of both the α and γ phase, because of the hybrid nature of the commercial material used; (ii) after the 150°C treatment, the intensity of the peaks due to the γ phase were reduced, with a corresponding increase of the ones relative to α. This observation is in agreement with what reported in Ref. 9 and it can be explained by the γ→ε phase transition at 150 °C, where ε-$Mg(BH_4)_2$ is converted in α phase after quenching at RT. (iii) At 190°C, the pattern was characterized by the presence of residual signals relative to the α phase and it was dominated by the peaks of one or more new crystalline phases of $Mg(BH_4)_2$, not previously reported (the interplanar spacing, diffraction angle and relative intensity of diffraction peaks for unidentified phases are listed in Table S1 in the Supporting Information). In fact, on the basis of the spectroscopic results that ruled out the formation of some decomposition products and of the XRD pattern at 200 °C (see below), it can be affirmed that long annealing at this temperature leads to a further phase transition in $Mg(BH_4)_2$. In particular, the γ→ε transformation was completed and followed by ε → phase(I) with the simultaneous α → phase(II): a difference in the phases originating from γ and α phases cannot be excluded, although phase(II) can be coincident with phase(I). In the following these two phases will be indicated with the comprehensive name of υ phase. (iv) At 200 °C the pattern was dominated by the peaks of the β' phase, which has been reported previously[9, 12, 17] as an intermediate phase during decomposition. This phase has been suggested with an orthorhombic structure with I*mmm* space group by Her et al.[13] and Filinckuk et al.[20] or I222 or extinction equivalent by Paskevicius et al.[9] β' reflections can be easily obtained from those of the β phase considering the extinction of the odd h,k,l reflections due to significant antisite disorder.[13] For this reason, this phase has been named β' in Ref. 17. The

corresponding body-centered cell is equivalent to 1/8 of the Fddd cell.[9, 13] As an example, from the peaks position, a cell dimension with a = 18.575 Å, b = 9.302 Å and c = 5.458 Å has been obtained for the sample annealed at 200 °C in H_2, that are almost coincident with those already reported for the I*mmm* cell of β'.[13] (v) At 205°C, the pattern is still dominated by the β' phase peaks, but a broad halo at 14° (d = 6.32 Å) appears: this broad signal has been associated in literature to amorphous $Mg(BH_4)_2$ formed after quenching at RT of melted $Mg(BH_4)_2$.[2, 9] Nevertheless, being observed at temperatures sensitively lower than the melting temperature of $Mg(BH_4)_2$, this peak can be likely associated to the products of the early stages of the decomposition, as expected on the basis of the weight loss observed at this temperature (see Table 1). In fact, the occurrence of amorphous halos in the XRD pattern during decomposition of $Mg(BH_4)_2$ has been already reported.[9, 12, 17, 36] A summary of these signals reported as the corresponding scattering vectors k ($k = 4\pi\sin\theta/\lambda$) is given in Table S2. It is interesting to notice as halos at d = 6.2-6.5 Å have been previously reported along the decomposition of $Mg(BH_4)_2$,[9, 12, 36] and associated with the beginning of the dehydrogenation process. The origin of this halo can be associated to a local change in the microstructure of the material because of the formation of reaction intermediates. In fact, it can be expected that the decomposition reaction would starts simultaneously in different zones of the material, originating crystalline grains of smaller dimensions with respect to the starting ones. Because of that, the corresponding diffraction peaks are quite large, leading to the appearance of halos. An indication of that can be seen in the fact that MgH_2 as decomposition products for temperature lower than 250 °C, is clearly identifiable in the IR spectra (see below) whereas its presence by using only XRD cannot be clearly stated. Only at higher temperatures, where crystal growth occurs, the observation of MgH_2 XRD peaks in the pattern becomes clear. Recently a similar result was reported by Yan et al.[10] for T =265 °C. Beside the work in Ref. 36, where this signal is observed at 200-225 °C, this halo was reported only at higher temperatures: 295[12] and 325 °C.[9] This difference in the temperature at which the decomposition starts can be easily explained on the basis of the different approach used previously and in the present work. It is interesting to notice that, on the contrary, in

the work of Guo et al.[36] the decomposition started at 200-225 °C although the sample was decomposed by using a thermal ramp of 2 °C min^{-1}, and then in conditions far from the near-equilibrium ones adopted here. In fact, in this study, $Mg(BH_4)_2$ was ball milled before decomposition, then facilitating the dehydrogenation rate also at low temperature.[36] The assignment of the halo at 14° to decomposition products is here supported also by the appearance of new bands in the infrared spectrum (see below), previously assigned to dehydrogenation species.[2] The dehydrogenation products in the pre-melting temperature range are likely different from the ones characterizing the post-melting temperature range and they will be indicated in the following as Mg-B-H(I). (vi) Up to 225 °C, a simultaneous increase in the intensity both of the halo at 14° and of the peaks associated to the β' phase is observed. (vii) At 250 °C, the intensity of the β' phase peaks results to be significantly decreased. In the **H2** sample, the intensity of the halo at 14° reaches its highest value, whereas in the **vac** sample it seems to be partially reduced with respect to what observed in the pattern obtained after a treatment at 225 °C: this difference can be explained on the basis of the partial sublimation of the material in vacuum at this temperature that might cause the partial removal of some decomposition products. Considering the maximum of the amorphous halo as an evidence of the average interplanar spaces, a value corresponding to 6.32 Å turns out for the peak at 14°, in good agreement with the value of 6.50 Å observed in Ref. 12 at slightly higher temperatures. (viii) At 300°C, the 14° halo strongly decreased in intensity in both the **vac** and **H2** patterns (with a stronger decrease registered for the **vac** sample), with the simultaneous appearance of three broad halos at 42, 62 and 77 degrees, as already observed in Refs. 12, 17, 36 at similar temperatures (see Table S2). The assignment of these signals is also not trivial: in fact, they can be associated to the formation of MgO due to the presence in the starting material of small traces of borates,[2, 24, 36] but also[36] to MgB_2, or to generic B-rich species (Mg-B-H(II), that is to the first dehydrogenation intermediates in the post-melting region). Because of the large FWHW of the corresponding halos, nothing can be inferred on the structure of these intermediates, that can be different after **vac** and **H2** treatments. For that reason, they are indicated with a different notation in

the following, that is as Mg-B-H(IIv) and Mg-B-H(IIh), respectively. Besides these broad signals, only in the XRD pattern registered for the sample treated in vacuum the peaks of elemental Mg are recognizable whereas, for the sample annealed in hydrogen, MgH_2 signals are evident. This difference was already reported by Hanada et al.[24] (ix) At 400 °C, the halo at 14 degrees completely disappeared in both samples while the halos at 42, 62 and 77 degrees became more evident. This would correspond to an increase in the concentration of MgO or MgB_2 or to the further dehydrogenation of Mg-B-H(II) to Mg-B-H-(III) species. In the **H2** treated sample, the peaks of MgH_2 are substituted by those of elemental Mg, characterized by a very small FWHW. On the contrary, in the **vac** treated sample the peaks of Mg were not present anymore after the treatment at 400 °C because of the almost complete sublimation of elemental Mg in these conditions.

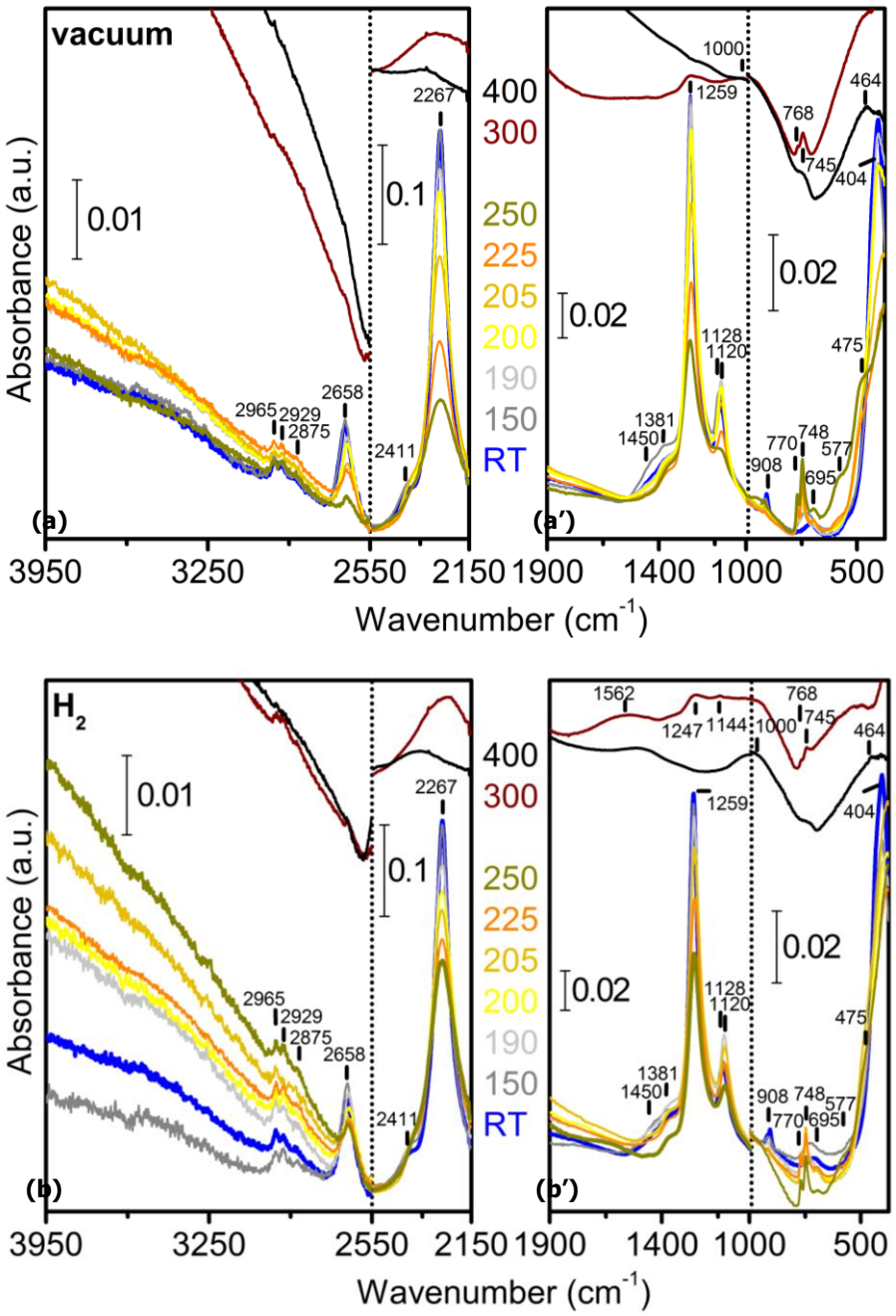

Figure 3. FTIR spectra recorded in the MIR after thermal decomposition of γ-$Mg(BH_4)_2$ in the RT-400 °C range (a, a') in dynamic vacuum ($p < 10^{-3}$ mbar) and (b, b') in hydrogen atmosphere (p = 300 mbar) on loose powder in ATR. The color legend referring to the decomposition temperature (in Celsius) is reported in the graph.

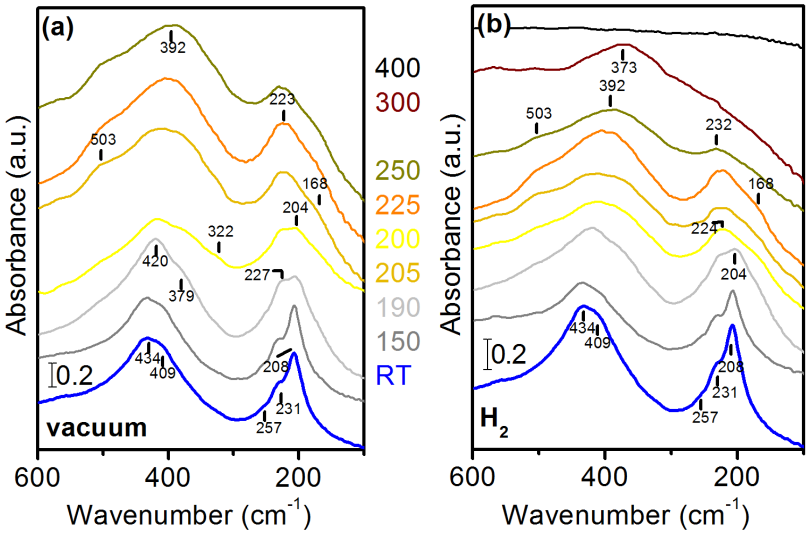

Figure 4. FTIR spectra in FIR recorded after thermal decomposition of γ-$Mg(BH_4)_2$ in the RT-400 °C range (a) in dynamic vacuum ($p < 10^{-3}$ mbar) and (b) in hydrogen atmosphere (p = 300 mbar) on diluted samples in wax, measured in transmission. The color legend referring to the decomposition temperature (in Celsius) is reported in the graph.

FTIR spectroscopy. Infrared spectra of γ-$Mg(BH_4)_2$ decomposed in **vac** and **H_2** atmosphere are reported in Figure 3 (upper and lower part, respectively) for the medium infrared region (3950-375 cm^{-1}, MIR) and in Figure 4 for the far infrared region (400-100 cm^{-1}, FIR, a and b, respectively). At RT, the spectrum of $Mg(BH_4)_2$ in the MIR (blue line in Figure 3a and 3a') is dominated by two strong signals at 2267 and 1259 cm^{-1} due to the B-H stretching and bending modes, respectively.[2, 3, 37, 38] Less intense signals are present at about 2900 cm^{-1} (likely due to residual solvent $S(CH_3)_2$ in the pores of γ-$Mg(BH_4)_2$), 2658, 1458, 1381, 1120, 908 and 700 cm^{-1} (see Table 2 for all the assignments). It is important to stress as the intensity of the bands relative to solvent impurities is two orders of magnitude lower than those relative to B-H stretching and bending signals, allowing to consider negligible their concentration in the sample (see Figure S3 for a more direct comparison). Another strong signal is observed at about 400 cm^{-1}, likely associated with Mg-B vibrations. For what concerns the **vac** treated samples, heating does not cause changes in the spectrum up to 200 °C, where a small decrease in the intensity of B-H band is observed, suggesting the beginning of $Mg(BH_4)_2$ dehydrogenation. At this temperature, the XRD patterns showed the

appearance of the broad halo at 14° that can be then associated to the amorphous products of the material decomposition for $T < 270$ °C. Starting from 205 °C and up to 250 °C, all the IR features associated to $Mg(BH_4)_2$ modes decrease gradually in intensity, clearly indicating the decrease in the concentration of B-H species with increasing temperature due to dehydrogenation. Together with the decrease of intensity of IR peaks related to B-H containing compounds, the growth of a doublet at 770 and 748 cm^{-1}, with a shoulder at 695 cm^{-1} is observed. This doublet is then likely the infrared fingerprints of Mg-B-H(I) species, as previously suggested.[2, 3] After rehydrogenation, the disappearance of these infrared bands was observed,[2] indicating Mg-B-H(I) species as the ones at the basis of the ability of $Mg(BH_4)_2$ to reversibly hydrogenate. Nevertheless, these Mg-B-H(I) species have not been fully identified yet.[2, 3] It is important to notice as the doublet at about 2550 cm^{-1} reported for the $Mg(B_3H_8)_2$ compound,[39] indicated by ^{11}B NMR in D_2O[1, 3] and DMSO-d_6 as the main Mg-B-H(I) species,[10] is absent in the spectra reported in Figure 3, suggesting to rule out the formation of this compound in the dehydrogenation of $Mg(BH_4)_2$ in the conditions adopted in this study. IR measurements were not able to unambiguously confirm the presence of $(B_3H_8)^-$ species in the dehydrogenated samples in a combined NMR/IR study.[3] Moreover, a recent computational work using the CALPHAD method, suggested as unfavoured from a thermodynamic point of view, the dehydrogenation of $Mg(BH_4)_2$ to $Mg(B_3H_8)_2$.[21] At 250 °C, IR signals that can be associated to the formation of MgH_2 can be clearly observed (Figure 3a') at 1120, 959, 475 cm^{-1} (see Figure S3). At T =300 °C, the spectrum shows a drastic change in the baseline indicative of a strong modification in the chemical nature of the material, as already evidenced by XRD characterization. In particular, the B-H signals are almost completely disappeared. The doublet at about 750 cm^{-1} observed in the IR spectrum of the sample annealed at 250 °C is strongly decreased in intensity with an inversion in the intensity and a slight shift of the peaks at 770 and 748 cm^{-1}. The changes of those signals can be indicative of a change in the local environment around the Mg-B-H(I) species or, more likely, to their further dehydrogenation to Mg-B-H(IIv). New signals at 1000 and 464 cm^{-1} appear, associable to MgB_2 species.[40] The presence of MgO cannot be ruled out from

those spectra, being characterized by a broad band at 425 cm^{-1}.[26] Alternatively, these four signals can be all associated to Mg-B-H(IIv) species. At 400 °C, the spectrum (black curve) is further simplified, presenting only four signals at about 2300, 1000, 745, 464 and 400 cm^{-1}. These features can be associated either to MgO/MgB_2 or to (one or more) Mg-B-H(IIIv) species obtained from the dehydrogenation of Mg-B-H(IIv).

Table 2. Vibrational frequencies assignment of the γ-$Mg(BH_4)_2$ at RT.

frequency (cm^{-1})	**assignments**
2900	solvent
2658	overtones[2]
2411	combination mode[37]
2267	B-H stretching[37]
1458, 1381, 1259, 1120	B-H bending[37]
908, 700	borates[2] or combination modes
434, 409	Mg-B vibrations[2, 26]
257, 231, 208	B-Mg-B bending[26]

For what concerns samples annealed in **H2**, in the MIR spectra (Figure 3b and 3b') they show a behavior similar to that observed for the corresponding samples treated in **vac** for $T < 270$ °C. Up to 250 °C, the main difference between the samples treated in **vac** with respect to those treated in **H2** is the smaller decrease of the intensity of the $Mg(BH_4)_2$ signals and a lower intensity of the bands associated to the decomposition products (both Mg-B-H(I) and MgH_2). At 300 °C, MgH_2 bands (in accordance with the XRD analysis) and a peak at 1562 cm^{-1}, not present in the corresponding sample annealed in **vac**, can be evidenced. The latter signal can be considered as a fingerprint of Mg-B-H(IIh) species. In the spectrum recorded after the treatment at 400 °C, this signal is shifted at about 1400 cm^{-1}, likely because of the further dehydrogenation of the Mg-B-H(IIh) to Mg-B-

H(IIIh). Moreover, a disappearance of MgH_2 signals was observed because of its dehydrogenation to Mg, as already observed in XRD characterization.

For what concerns the far infrared region (parts a and b of Figure 4 for **vac** and **H2** samples, respectively), all the spectra were characterized by two main band groups, centered at 400 and 200 cm^{-1}. These groups have been previously associated to Mg-B stretching and B-Mg-B bending.[26, 41] They can be also associated to other stretching and bending modes (B-B stretching, out of plane ring bending, etc.) if B-B covalent bonds are present in the decomposition products (see for example Table S4). The spectra in the FIR region showed a larger dependence on the temperature than observed in MIR. In particular, whereas in the MIR, up to 200 °C essentially no changes are observed in the spectral features, in FIR the two complex bands at about 400 and 200 cm^{-1} observed at RT (blue line) undergoes in the RT ≤ T ≤ 190 °C temperature range to a strong change in shape and position. In particular the band at 200 cm^{-1} has been reported to be a particularly good fingerprint of different $Mg(BH_4)_2$ isomorphs.[26] This observation might be useful for the identification of the unidentified new phase of $Mg(BH_4)_2$ evidenced in the XRD characterization (υ phase) in future works combining structural Rietveld refinement and periodic quantum mechanical calculations. For what concerns the evolution of the spectra for 200 ≤ T ≤ 250 °C, several signals appear, whose identification was in most of the cases not possible on the basis of the data available in the literature. For T > 270 °C, the description of the reaction evolution is coincident with the one reported above for the MIR part of the spectra.

UV-Vis-NIR analysis basically support the results obtained by MIR also in the NIR (see Supplementary Information), indicating a decrease of the BH_4 overtones starting from 200°C. For what concern the UV-Vis region, an increase in the band gap of the material is observed upon increasing the temperature, as suggested by the change in the color of the samples after the annealing.

DISCUSSION

The amorphous nature of the Mg-B-H species (likely due to the local character of the decomposition process, especially for $T < 270$ °C) makes particularly difficult their identification by means of diffraction techniques. Moreover, the infrared spectra of all the possible intermediates species have not been reported so far. For this reason, a possible assignment of the IR features reported above has been attempted by coupling the spectroscopic characterization with a density functional study. In particular, the investigation of the Mg-B-H(I) species has been carried out, being the ones responsible for the rehydrogenation of $Mg(BH_4)_2$ in mild conditions.[2, 9, 42, 43] All the spectral features obtained for the decomposition products in the pre-melting temperature range were then used to assess the results of a quantum mechanical screening of the most likely candidates as Mg-B-H-(I) species, accordingly to the literature.[2, 9, 42, 43] In this study, a screening of the possible Mg-B-H(I) candidates has been carried out by considering only the part involving covalent bonds, that is B-B and B-H bonds (i.e. for the ionic candidates, considering only the anionic moiety). These bonds are in fact the ones dominating the MIR spectra. Among the systems proposed in literature,[42-44] only those characterized by a high H/B ratio have been considered. In fact, the asymptotic mass loss at 250°C was estimated to be only 2.94 mass% for the decomposition in hydrogen atmosphere (see Figure 1). The value obtained for decomposition in vacuum has not been considered being largely affected by sublimation. On the basis of the TGA-MS study conducted by David et al.,[17] about 0.5 mass% can be also associated to B_2H_6 or solvent evolution from the sample. The total mass loss at 250°C can be then estimated between 2.4 and 2.9 mass%. The clusters adopted for the calculations are reported in Figure 5: $[B_2H_6]^{2-}$,[43] $[B_2H_7]^{-}$,[42] $[B_3H_6]^{3-}$,[42] $[B_3H_7]^{2-}$,[42] $[B_3H_8]^{-}$,[42] $[B_5H_9]$[44, 45] and $[B_5H_{11}]$.[44] $Mg(BH_4)_2$ has been simulated by means of the $[BH_4]^{-}$ unit, that is with the same approximation adopted for the reaction products, in order to allow the comparison of the spectroscopic data on the basis of bands shift. $[B_{12}H_{12}]^{2-}$ and $[B_{10}H_{10}]^{2-}$ anions were also considered because $[B_{12}H_{12}]^{2-}$ and $[B_{10}H_{10}]^{2-}$ species have been identified after $Mg(BH_4)_2$ decomposition in different temperature and pressure conditions.[2, 46] The simulated IR spectra of these systems, along

their optimized coordinates and HOMO-LUMO energy difference are reported in the Supporting Information. In order to evaluate the ability of the adopted computational approach to correctly simulate the vibrational modes of the Mg-B-H species, the calculated modes have been compared with the corresponding experimental values reported in the literature for the species for which such data exist. This comparison indicated as the simulated frequencies are in good agreement with the experimental values, with an error lower than 10%. For example, the simulated spectrum for $[B_{12}H_{12}]^{2-}$ is constituted by three main peaks at 2515, 1064 and 704 cm^{-1} (see Figure S11) that agree with the bands experimentally reported at 2470, 1070 and 720 cm^{-1}.[3] It is important to stress that it has been proposed in the literature that the reversible phase could be also constituted by polymeric forms of the species considered in the DFT screening here proposed.[10] The present study would not allow to distinguish between monomeric and polymeric form of the borane species but only to rule out their presence, independently on their monomeric or polymeric form.

Considering all the simulated spectra (Figures S5-S8), it can be noticed that only some of them show IR peaks in the region between 800 and 600 cm^{-1} ($[B_3H_8]^-$, B_5H_9, $[B_2H_7]^-$, $[B_3H_7]^{2-}$, $[B_5H_{11}]$, $[B_{10}H_{10}]^{2-}$ and $[B_{12}H_{12}]^{2-}$). Nevertheless, none of the clusters considered is able to correctly fit all the changes observed in the IR spectrum after treatment at 250 °C (dark yellow curves in Figure 3) and then to represent a good candidate for Mg-B-H(I). In fact, $[B_3H_8]^-$, $[B_2H_7]^-$, $[B_{10}H_{10}]^{2-}$ and $[B_{12}H_{12}]^{2-}$ show peaks at significantly higher wavenumbers with respect to the B-H stretching band in $Mg(BH_4)_2$, in contrast to what observed experimentally for Mg-B-H(I) (see Figure S5-S8). Moreover, B_5H_9, $[B_3H_7]^{2-}$ and $[B_5H_{11}]$ clusters show absorbance bands at about 1500 cm^{-1} not present in the experimental spectra, allowing to also rule out their presence in the material decomposed at 250 °C. Although the simulation of the band gap of a material by using the HOMO-LUMO difference is a quite rough approximation because of the cluster models adopted, it is worth noticing that, for what concerns $[B_3H_8]^-$, B_5H_9 and $[B_2H_7]^-$, they were also unable to reproduce the

red shift in the band gap after decomposition observed in the experimental UV-Vis spectra (see Figure S2 in the Supporting Information).

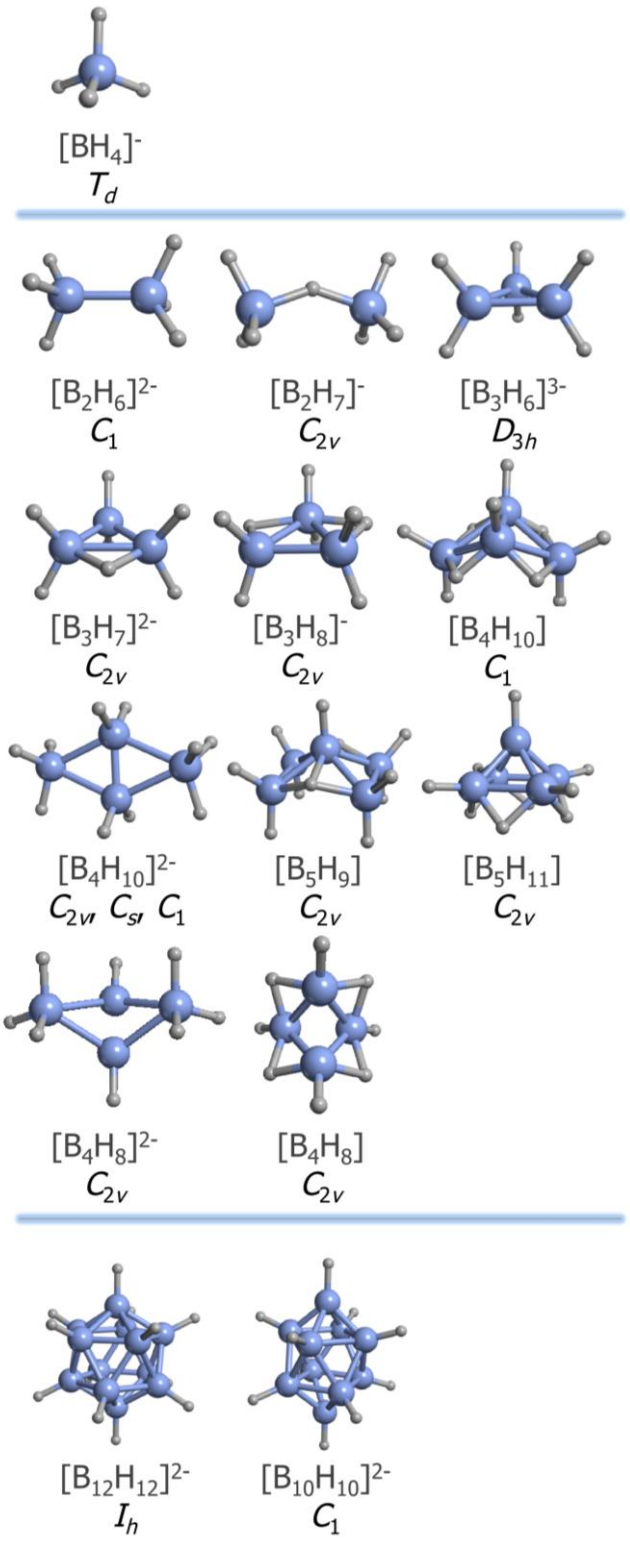

Figure 5. [B_nH_m]$^{q-}$ clusters used to simulate the possible Mg-B-H(I) intermediates. The structures reported have been optimized at the B3LYP/TZVp level. The symmetry of each cluster in its minimum configuration is reported. For $[B_4H_{10}]^{2-}$, the reported geometry is the one calculated imposing the C_{2v} symmetry constraint. Boron and hydrogen atoms are represented as blue and grey spheres, respectively.

Although none of these clusters was able to model the experimental spectra, the comparison of the experimental spectra with the calculated ones allow to identify some characteristics of the Mg-B-H(I) intermediates. (i) First of all, it is possible to associate the doublet peaks at 748 and 770 cm^{-1} to frustrated ring breathing modes. This means that the Mg-B-H(I) intermediates have to possess a ring structure (simple or complex), constrained in some way on at least one half of the ring sides. (ii) Terminal B-H bonds, giving signals at frequencies higher than the B-H stretching modes of $Mg(BH_4)_2$ have to be absent (on the contrary of what expected for Mg-B-H(II) and Mg-B-H(III) species). (iii) In addition, the presence of H bridged atoms on BH_n-BH_n sides of the ring (with n = 1 or 2) can be excluded in Mg-B-H(I) compounds, because showing signals at about 1500 cm^{-1} (observed on the contrary for Mg-B-H(IIh) and Mg-B-H(IIIh) species).

In order to hypothesized alternative decomposition products with respect to the ones reported in the literature for the pre-melting temperature range, some considerations have to be done on the structure of β'-$Mg(BH_4)_2$, the stable phase of $Mg(BH_4)_2$ at the beginning of its decomposition[2, 9] and atomically coincident[9] with β-$Mg(BH_4)_2$ (being a form of β-$Mg(BH_4)_2$ with significant antisite disorder)[13, 17] that is reported in Figure S1. The structure of β'-$Mg(BH_4)_2$ can be described as constituted by 4-rings of Mg-BH_4 units: the first decomposition step of $Mg(BH_4)_2$ could then likely bring to the formation of species which structure reminds to the parent structure. Tetraborane, characterized by a four ring geometry, is one of the first reported borane.[47] $Na_2B_4H_{10}$ and $K_2B_4H_{10}$ have been also reported.[48, 49] These two four-member ring species (anionic and neutral) have been then considered in the calculations. Because the only information available in the literature

regarding $Na_2B_4H_{10}$ suggests its possible decomposition at 170 °C to $Na_2B_4H_8$,[49] also $[B_4H_8]^{2-}$ and $[B_4H_8]$ have been modeled.[50] Nevertheless the presence of these two last species can be ruled out on the basis of the simulated IR spectrum, requiring bands at wavenumbers higher than 2550 cm^{-1} (see Figure S12) The optimized structures of $[B_4H_{10}]$ and $[B_4H_{10}]^{2-}$ are reported in Figure 5. In Figure 6, the experimental spectra obtained for γ-$Mg(BH_4)_2$ at RT and after thermal treatment at 250 °C (upper part, black and orange curves, respectively) are compared with that calculated for $[BH_4]^{2-}$ and $[B_4H_{10}]^{2-}$ (lower part, black and orange/dark yellow curves, respectively). At difference of its neutral counterpart, $[B_4H_{10}]^{2-}$ spectrum was in a very good agreement with the experimental one (see Figures S9 and S10 and Figure 6). Three different symmetries have been considered in the optimization of $[B_4H_{10}]^{2-}$, in order to have some additional information: C_1, C_s and C_{2v}. Because the spectra obtained for the C_1 and C_s conformers were essentially the same (see Figure S10), only the C_1 spectrum is reported in Figure 6 (lower part, dark yellow curve). The three symmetry constraints caused very slight changes in the atomic coordinates. Among the conformers considered, the one in C_{2v} symmetry gave the best fit to the experimental data. The calculations indicates as the C_{2v} conformer in the gas phase would be characterized by two imaginary modes, that is it does not constitute a minimum geometry at difference of the clusters having C_1 and C_s symmetry. Nevertheless, it is possible that the C_{2v} conformer is stabilized in the solid state. In fact, the energy difference between the C_{2v} and C_1 conformers has been estimated to be of only 10 kJ mol^{-1}. By comparison of the experimental spectra with the theoretical ones, the presence of both the conformers can be in fact considered. It is also worth of noticing that the experimental band width observed for both pristine and decomposed $Mg(BH_4)_2$ is quite large. In particular, before decomposition the FWHM of the stretching and bending modes in $Mg(BH_4)_2$ is of about 15 and 40 cm^{-1}, respectively. These peaks are further broadened after decomposition at 250 °C (FWHM of 190 and 120 cm^{-1}, in vacuum) likely because of the simultaneous presence of different conformers of the decomposition products. In Figure 6 a FWHM of 25 cm^{-1} has been adopted for the calculated spectra in order to allow to better appreciate the differences between the various species.

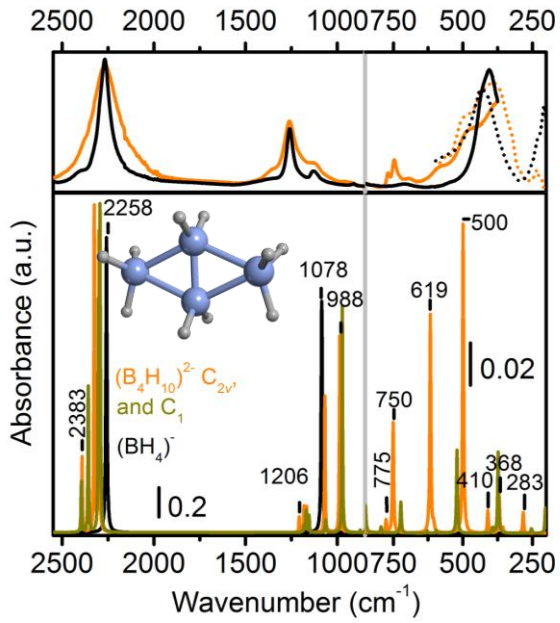

Figure 6. Top: IR spectra of γ-$Mg(BH_4)_2$ before (black lines) and after thermal decomposition at 250 °C for 20 h in dynamic vacuum ($p < 10^{-3}$ mbar, orange lines). The spectra have been normalized in order to facilitate the comparison. Solid lines: ATR-MIR spectra; Dotted lines: FIR spectra. **Bottom:** calculated IR spectra at the B3LYP/TZVp level for the $(BH_4)^-$ unit (black line) and the $(B_4H_{10})^{2-}$ anion in C_{2v} and C_1 geometry (orange and dark yellow lines, respectively).

The formation of $[B_4H_{10}]^{2-}$ species in the first step of the decomposition process would ask for the reaction:

$2\ Mg(BH_4)_2 \rightarrow MgB_4H_{10} + MgH_2 + 2\ H_2$

that is characterized by a 3.7 mass% loss due to hydrogen evolution (see Table S3). This value is only slightly higher than the mass loss of 2.4-2.9 mass% measured experimentally in the TGA analysis. This difference can be related to the underestimation of the asymptotical decomposition amount in the experiments because of the slow decomposition kinetics. Decomposition of $Mg(BH_4)_2$ at temperature slightly larger than $Mg(BH_4)_2$ melting temperature (280-285 °C and 2.7 bar of hydrogen monitored for 20 h in a volumetric apparatus) provided a mass loss of 4.1 mass%.[2] The material was able to reabsorb 2.1 mass% of hydrogen in mild conditions (280-285°C and 115-125 bar for 16 h).[2] The rehydrogenable fraction was then lower than the theoretical value of 3.7 mass%. A fast cycling of the material was also observed and it can be likely associated to the

working temperature adopted in that study: in fact, being slightly larger than the melting temperature of the borohydrides, it would facilitate on one hand the separation of the different decomposition products (reported to happen in these conditions and to cause the separation between B-rich and Mg-rich by-products, that is between boranes and MgH_2/Mg)[9] and, on the other hand, the formation of $[B_{10}H_{10}]^{2-}$ and $[B_{12}H_{12}]^{2-}$ species.[2, 9, 10, 51] Both these factors have been reported to be at basis of the high difficulty in rehydrogenation of $Mg(BH_4)_2$ after a decomposition at *T* significantly higher than 270°C.[9]

Although outside the aim of the present study because not all the possible alternative products were considered for $T > 270$ °C, in agreement with previous reports,[46, 51] it is interesting to notice that $[B_{10}H_{10}]^{2-}$ and $[B_{12}H_{12}]^{2-}$ were the only two species that provided a good fit of the spectrum obtained after decomposition in vacuum at 300 and 400 °C (Mg-B-H(IIv) and Mg-B-H(IIIv) species) and in hydrogen at 400 °C (Mg-B-H(IIIh)). The comparison, reported in Figure S11, is particularly good for $[B_{12}H_{12}]^{2-}$. For what concerns the sample decomposed in dynamic vacuum, the presence of $[B_{12}H_{12}]^{2-}$ has been recently ruled out for decomposition temperatures in the range 265-400 °C on the basis of NMR and IR spectroscopies, allowing to hypothesize the presence of polymeric $Mg_{2m}[B_3H_7\text{-}B_nH_n]_m$ species (with $6 \leq n \leq 12$).[10] For what concerns IR, it is expected that the bands of $[B_nH_n]^{2-}$ in the polymeric form would be very close to the ones in the monomeric form. Although, as stated above, this study is focused only on the pre-melting temperature range, it can be here proposed that *n* equal to 12 would be the most abundant species in the polymer proposed. For what concerns the decomposition in hydrogen at 300 °C, the fingerprints of Mg-B-H(IIh) is the peak at 1562 cm^{-1} (see Figure 3b). In this case, the formation of $[B_4H_8]^{2-}$, B_5H_9 or B_5H_{11} could be also considered (see Figure S5-S11) but further investigations are needed in order to shed some light on the by-products obtained for decomposition of $Mg(BH_4)_2$ at *T* higher than the melting temperature.

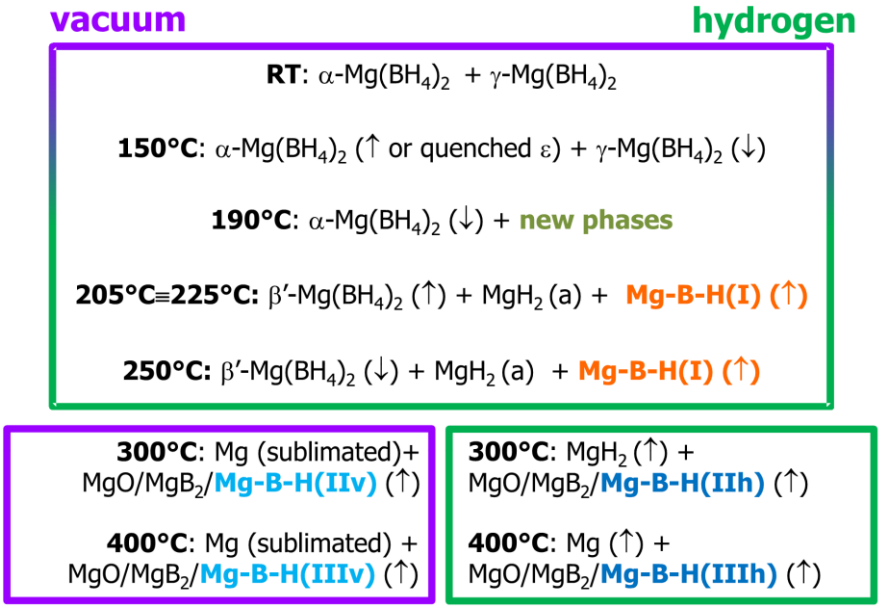

Scheme 1. Dehydrogenation process of γ-$Mg(BH_4)_2$ in dynamic vacuum and in H_2 atmosphere, where Mg-B-H(I) = MgB_4H_{10}. ↑ = increase in the concentration of the species with respect to the previous temperature step; ↓ = decrease in the concentration of the species with respect to the previous temperature step.

CONCLUSIONS

The dehydrogenation process of γ-$Mg(BH_4)_2$ has been characterized in this study by considering two well defined reaction environments, dynamic vacuum and hydrogen atmosphere. At difference of previous reports, the slow rates of $Mg(BH_4)_2$ decomposition have been taken into account by considering very long reaction time. Moreover, a particular attention has been paid to the dehydrogenation process in the pre-melting temperature range, because it has been reported to be a reversible process in conditions interesting on the applicative point of view. The conclusions of the present work are summarized in Scheme 1, where it is reported the proposed decomposition paths of $Mg(BH_4)_2$ in dynamic vacuum and hydrogen atmosphere, as obtained by the combined analysis of the literature data and of those obtained in the present multi-technical approach.

Far to be comprehensive, this study has nevertheless allowed to clarify several points debated in the literature on this process. In particular: (a) the starting temperature of the $Mg(BH_4)_2$ dehydrogenation in the near-equilibrium conditions here adopted was identified to be 200 °C, on the basis of both XRD and IR analyses, that is a temperature significantly lower than the melting temperature of the material. (b) MgB_4H_{10} was proposed as a plausible candidate for the species at the basis of the ability of $Mg(BH_4)_2$ to rehydrogenate in mild conditions (Mg-B-H(I)). The identification of this species was possible by the combined use of infrared spectroscopy and density functional theory. Future studies aimed to the synthesis and characterization of $Mg_2B_4H_{10}$ will allow to definitely confirm or rule out this compound as the reversible intermediate in the decomposition of γ-$Mg(BH_4)_2$. (c) The existence of a new $Mg(BH_4)_2$ isomorph, which structure is at present unresolved, has been evidenced at 190 °C. (d) MgH_2 was identified to be an important decomposition product already in the first steps of the material dehydrogenation, both in hydrogen atmosphere and in vacuum. Because amorphous, its identification was possible only by means of infrared spectroscopy. Its presence was previously suggested (see for example refs. 9 and 10) but its unambiguous identification was possible here because of the infrared spectra with higher resolution than those reported in the literature so far[9, 10] for the pre-melting temperature range.

Interestingly, an important sublimation of the decomposition products was directly observed in vacuum at difference of what observed in hydrogen atmosphere: this observation suggests that dehydrogenation in vacuum of complex hydrides causes a fast degradation of the material and it has then to be avoided. This is a valuable information on the applicative point of view. Moreover, it also suggests that particular care have to be adopted when the analysis of gravimetric decomposition in vacuum is carried out in order to identify temperature ranges possibly affected by sublimation.

In the end, from this study, it seems evident that if the possibility to rehydrogenate $Mg(BH_4)_2$ in mild conditions is related to the formation of Mg-B-H(I) intermediates (as it has been suggested in the literature),[1, 2] the hydrogen amount that can be easily reversible in $Mg(BH_4)_2$ would be then restricted to 3.7 mass% (see Table S3), without any possibility to increase it by material

modification. In order to make $Mg(BH_4)_2$ a material more interesting for hydrogen storage then, strategies aimed to allow the reversibility of the dehydrogenation process in the post-melting temperature range have to be foreseen, contemplating the avoiding of the phase separation and formation of closoboranes.

ASSOCIATED CONTENT

Supporting Information. Schematic review of $Mg(BH_4)_2$ decomposition open points; discussion on the structure of $Mg(BH_4)_2$ polymorphs; XRD patterns: additional details; DR-UV-Vis spectroscopy results; ATR-MIR of γ-$Mg(BH_4)_2$ before and after decomposition; ATR-MIR spectrum of MgH_2; Theoretical mass loss for the formation of different Mg-B-H intermediates; Assignment of the bands in the theoretical IR spectrum of $[B_4H_{10}]^{2-}$ unit; Theoretical IR spectra of all the clusters; Atomic coordinates, HOMO-LUMO, energy of all the clusters as obtained at the B3LYP/TZVp level. This material is available free of charge via the Internet at http://pubs.acs.org.

AUTHOR INFORMATION

Corresponding Author

* Department of Science and High Technology, Università dell'Insubria, Via Valleggio 11, 22100 Como, Italy. Tel.: +39 031-2386614, Fax: +39 031-2386630, E-mail: jenny.vitillo@uninsubria.it.

ACKNOWLEDGMENTS

Fabio Lepore and Lorenzo Grimaldi are acknowledged for the help in the experiments. Dr. Olena Zavorotynska, Dr. Stefano Deledda, Dr. Elisa Albanese and Dr. Bartolomeo Civalleri are acknowledged for useful discussions. Dr. Elena Groppo is acknowledged for the help for the far infrared measurements. Financial support by the European Fuel Cells and Hydrogen Joint Undertaking through the BOR4STORE project (grant n. 303428) is acknowledged.

ABBREVIATIONS

XRD, X-Ray Powder Diffraction; FTIR, Fourier-transformed infrared; NIR, near infrared; MIR, medium infrared; FIR, far infrared; ATR, Attenuated Total Reflectance; DR-UV, diffuse reflectance spectroscopy in the UV-Visible spectral range; DFT, Density Functional Theory, Mg-B-H, B-containing decomposition intermediates of unknown composition.

REFERENCES

1. Chong, M.; Karkamkar, A.; Autrey, T.; Orimo, S.-i.; Jalisatgid, S.; Jensen, C. M., Reversible Dehydrogenation Of Magnesium Borohydride To Magnesium Triborane In The Solid State Under Moderate Conditions. *Chem. Commun.* **2011,** *47*, 1330–1332.
2. Zavorotynska, O.; Saldan, I.; Hino, S.; Humphries, T. D.; Deledda, S.; Hauback, B. C., Hydrogen Cycling In γ-$Mg(BH_4)_2$ With Cobalt-Based Additives. *J. Mater. Chem. A* **2015,** *3*, 6592-6602.
3. Saldan, I.; Hino, S.; Humphries, T. D.; Zavorotynska, O.; Chong, M.; Jensen, C. M.; Deledda, S.; Hauback, B. C., Structural Changes Observed during the Reversible Hydrogenation of $Mg(BH_4)_2$ with Ni-Based Additives. *J. Phys. Chem. C* **2014,** *118*, 23376-23384.
4. Pitt, M. P.; Webb, C. J.; Paskevicius, M.; Sheptyakov, D.; Buckley, C. E.; Gray, E. M., In Situ Neutron Diffraction Study of the Deuteration of Isotopic (MgB_2)-B-11. *J. Phys. Chem. C* **2011,** *115*, 22669-22679.
5. Severa, G.; Ronnebro, E.; Jensen, C. M., Direct Hydrogenation of Magnesium Boride to Magnesium Borohydride: Demonstration of > 11 Weight Percent Reversible Hydrogen Storage. *Chem. Commun.* **2010,** *46*, 421-423.
6. Newhouse, R. J.; Stavila, V.; Hwang, S.-J.; Klebanoff, L. E.; Zhang, J. Z., Reversibility and Improved Hydrogen Release of Magnesium Borohydride. *J. Phys. Chem. C* **2010,** *114*, 5224-5232.
7. Chlopek, K.; Frommen, C.; Leon, A.; Zabara, O.; Fichtner, M., Synthesis and Properties of Magnesium Tetrahydroborate, $Mg(BH_4)_2$. *J. Mater. Chem.* **2007,** *17*, 3496-3503.
8. Albanese, E.; Kalantzopoulos, G. N.; Vitillo, J. G.; Pinatel, E.; Civalleri, B.; Deledda, S.; Bordiga, S.; Hauback, B. C.; Baricco, M., Theoretical and Experimental Study on $Mg(BH_4)_2$-$Zn(BH_4)_2$ Mixed Borohydrides. *J. Alloy. Compd.* **2013,** *580*, S282-S286.
9. Paskevicius, M.; Pitt, M. P.; Webb, C. J.; Sheppard, D. A.; Filsø, U.; MacA. Gray, E.; Buckley, C. E., In-Situ X-ray Diffraction Study of γ-$Mg(BH_4)_2$ Decomposition. *J. Phys. Chem. C* **2012,** *116*, 15231−15240.
10. Yan, Y.; Remhof, A.; Rentsch, D.; Zuttel, A., The Role of $MgB_{12}H_{12}$ in The Hydrogen Desorption Process of $Mg(BH_4)_2$. *Chem. Commun.* **2015,** *51*, 700-702.
11. Soloveichik, G. L.; Gao, Y.; Rijssenbeek, J.; Andrus, M.; Kniajanski, S.; Bowman, R. C., Jr.; Hwan, S.-J.; Zhao, J.-C., Magnesium Borohydride as a Hydrogen Storage Material: Properties and Dehydrogenation Pathway of Unsolvated $Mg(BH_4)_2$. *Int. J. Hydrogen En.* **2009,** *34*, 916-928.
12. Ban, V.; Soloninin, A. V.; Skripov, A. V.; Hadermann, J.; Abakumov, A.; Filinchuk, Y., Pressure-Collapsed Amorphous $Mg(BH_4)_2$: An Ultradense Complex Hydride Showing a Reversible Transition to the Porous Framework. *J. Phys. Chem. C* **2014,** *118*, 23402-23408.
13. Her, J.-H.; Stephens, P. W.; Gao, Y.; Soloveichik, G. L.; Rijssenbeek, J.; Andrus, M.; Zhao, J.-C., Structure Of Unsolvated Magnesium Borohydride $Mg(BH_4)_2$. *Acta Cryst. B* **2007,** *63*, 561-568.

14. Filinchuk, Y.; Richter, B.; Jensen, T. R.; Dmitriev, V.; Chernyshov, D.; Hagemann, H., Porous and Dense Magnesium Borohydride Frameworks: Synthesis, Stability, and Reversible Absorption of Guest Species. *Angew. Chem. Int. Ed.* **2011,** *50*, 11162 –11166.
15. Amieiro-Fonseca, A.; Ellis, S. R.; Nuttall, C. J.; Hayden, B. E.; Guerin, S.; Purdy, G.; Soulie, J. P.; Callear, S. K.; Culligan, S. D.; David, W. I. F., et al., A Multidisciplinary Combinatorial Approach For Tuning Promising Hydrogen Storage Materials Towards Automotive Applications. *Faraday Discuss.* **2011,** *151*, 369-384.
16. Richter, B.; Ravnsbaek, D. B.; Tumanov, N.; Filinchuk, Y.; Jensen, T. R., Manganese Borohydride; Synthesis and Characterization. *Dalton Trans.* **2015,** *44*, 3988-3996.
17. David, W. I. F.; Callear, S. K.; Jones, M. O.; Aeberhard, P. C.; Culligan, S. D.; Pohl, A. H.; Johnson, S. R.; Ryan, K. R.; Parker, J. E.; Edwards, P. P., et al., The Structure, Thermal Properties and Phase Transformations of the Cubic Polymorph of Magnesium Tetrahydroborate. *Phys. Chem. Chem. Phys.* **2012,** *14*, 11800–11807.
18. Bil, A.; Kolb, B.; Atkinson, R.; Pettifor, D. G.; Thonhauser, T.; Kolmogorov, A. N., Van der Waals Interactions in the Ground State of $Mg(BH_4)_2$ From Density Functional Theory. *Phys. Rev. B* **2011,** *83*, 224103.
19. Černý, R.; Filinchuk, Y.; Hagemann, H.; Yvon, K., Magnesium Borohydride: Synthesis and Crystal Structure. *Angew. Chem. Int. Ed.* **2007,** *46*, 5765-5767.
20. Filinchuk, Y.; Černý, R.; Hagemann, H., Insight into $Mg(BH_4)_2$ with Synchrotron X-ray Diffraction: Structure Revision, Crystal Chemistry, and Anomalous Thermal Expansion. *Chem. Mater.* **2009,** *21*, 925-933.
21. Pinatel, E. R.; Albanese, E.; Civalleri, B.; Baricco, M., Thermodynamic Modelling of $Mg(BH_4)_2$. *J. Alloy. Compd.* **2015,** *645, Supp. 1*, S64-S68.
22. Paskevicius, M.; Ley, M. B.; Sheppard, D. A.; Jensen, T. R.; Buckley, C. E., Eutectic Melting in Metal Borohydrides. *Phys. Chem. Chem. Phys.* **2013,** *15*, 19774-19789.
23. Gilbreath, W. P., The Vapor Pressure Of Magnesium Between 223° And 385 °C. *NASA technical note* **1965**, NASA TN D-2723.
24. Hanada, N.; Chopek, K.; Frommen, C.; Lohstroh, W.; Fichtner, M., Thermal Decomposition of $Mg(BH_4)_2$ Under He Flow and H_2 Pressure. *J. Mater. Chem.* **2008,** *18*, 2611-2614.
25. Yan, Y.; Li, H.-W.; Nakamori, Y.; Ohba, N.; Miwa, K.; Towata, S.-i.; Orimo, S.-i., Differential Scanning Calorimetry Measurements of Magnesium Borohydride $Mg(BH_4)_2$. *Mater. Trans.* **2008,** *49*, 2751-2752.
26. Vitillo, J. G.; Groppo, E.; Bardají, E. G.; Baricco, M.; Bordiga, S., Fast Carbon Dioxide Recycling by Reaction With γ-$Mg(BH_4)_2$. *Phys. Chem. Chem. Phys.* **2014,** *16*, 22482-22486.
27. Lutterotti, L.; Matthies, S.; Wenk, H.-R.; Schultz, A. S.; Richardson, J. W., Combined Texture and Structure Analysis of Deformed Limestone from Time-of-Flight Neutron Diffraction Spectra. *J. Appl. Phys.* **1997,** *81*, 594-600.
28. Lutterotti, L., *MAUD*, http://www.ing.unitn.it/~maud (accessed October 12, 2015).
29. Frisch, M. J.; Trucks, G. W.; Schlegel, H. B.; Scuseria, G. E.; Robb, M. A.; Cheeseman, J. R.; Scalmani, G.; Barone, V.; Mennucci, B.; Petersson, G. A., et al. *Gaussian 09*, Revision A.02; Gaussian, Inc.: Wallingford CT, 2009.
30. Becke, A. D., Density-Functional Thermochemistry 3. The Role of Exact Exchange. *J. Chem. Phys.* **1993,** *98*, 5648-5652.
31. Lee, C.; Yang, W.; Parr, R. G., Development of the Colle-Salvetti Correlation-Energy Formula Into a Functional of the Electron Density. *Phys. Rev. B* **1988,** *37*, 785-789.
32. Ahlrichs, R.; Furche, F.; Grimme, S., Comment on "Assessment of Exchange Correlation Functionals" [A.J. Cohen, N.C. Handy, Chem. Phys. Lett. 316 (2000) 160-166]. *Chem. Phys. Lett.* **2000,** *325*, 317-321.
33. Li, H. W.; Kikuchi, K.; Nakamori, Y.; Ohba, N.; Miwa, K.; Towata, S.; Orimo, S., Dehydriding and Rehydriding Processes of Well-Crystallized $Mg(BH_4)_2$ Accompanying With Formation of Intermediate Compounds. *Acta Materialia* **2008,** *56*, 1342-1347.

34. Stadie, N. P.; Callini, E.; Richter, B.; Jensen, T. R.; Borgschulte, A.; Züttel, A., Supercritical N_2 Processing as a Route to the Clean Dehydrogenation of Porous $Mg(BH_4)_2$. *J. Am. Chem. Soc.* **2014,** *136*, 8181-8184.
35. Capurso, G.; Agresti, F.; Crociani, L.; Rossetto, G.; Schiavo, B.; Maddalena, A.; Lo Russo, S.; Principi, G., Nanoconfined Mixed Li and Mg Borohydrides as Materials for Solid State Hydrogen Storage. *Int. J. Hydrog. Energy* **2012,** *37*, 10768-10773.
36. Guo, S.; Chan, H. Y. L.; Reed, D.; Book, D., Investigation of Dehydrogenation Processes in Disordered γ-$Mg(BH_4)_2$. *J. Alloy. Compd.* **2013,** *580, Supplement 1*, S296-S300.
37. Giannasi, A.; Colognesi, D.; Ulivi, L.; Zoppi, M.; Ramirez-Cuesta, A. J.; Bardají, E. G.; Roehm, E.; Fichtner, M., High Resolution Raman and Neutron Investigation of $Mg(BH_4)_2$ in an Extensive Temperature Range. *J. Phys. Chem. A* **2010,** *114*, 2788-2793.
38. Hagemann, H., FTIR Spectra of Borohydrides. http://www.unige.ch/sciences/chifi/?ftirdb.html (accessed October 12, 2015).
39. Kim, D. Y.; Yang, Y.; Abelson, J. R.; Girolami, G. S., Volatile Magnesium Octahydrotriborate Complexes as Potential CVD Precursors to MgB_2-Synthesis and Characterization of $Mg(B_3H_8)_2$ and Its Etherates. *Inorg. Chem.* **2007,** *46*, 9060-9066.
40. Alarco, J. A.; Chou, A.; Talbot, P. C.; Mackinnon, I. D. R., Phonon Modes of MgB_2: Super-Lattice Structures and Spectral Response. *Phys. Chem. Chem. Phys.* **2014,** *16*, 24443-24456.
41. Nibler, J. W., Infrared and Raman Spectra of Gaseoux and Matrix Isolated Beryllium Borohydride. *J. Am. Chem. Soc.* **1972,** *94*, 3349-3359.
42. Zhang, Y.; Majzoub, E.; Ozoliņš, V.; Wolverton, C., Theoretical Prediction of Metastable Intermediates in the Decomposition of $Mg(BH_4)_2$. *J. Phys. Chem. C* **2012,** *116*, 10522−10528.
43. Zhang, Y.; Majzoub, E.; Ozolins, V.; Wolverton, C., Theoretical Prediction of Different Decomposition Paths for $Ca(BH_4)_2$ and $Mg(BH_4)_2$. *Phys. Rev. B* **2010,** *82*, 174107.
44. Lipscomb, W. N., *Boron Hydrides.* Dover Publications: 2012.
45. Bridgeman, A. J.; Empson, C. J., Detecting Delocalization. *New J. Chem.* **2008,** *32*, 1359–1367.
46. Remhof, A.; Yan, Y. G.; Rentsch, D.; Borgschulte, A.; Jensen, C. M.; Zuttel, A., Solvent-Free Synthesis and Stability of $MgB_{12}H_{12}$. *J. Mater. Chem. A* **2014,** *2*, 7244–7249.
47. Stock, A.; Massenez, C., Borwasserstoffe. *Ber. deutsch. chern. Ges.* **1912,** *45*, 3539-3568.
48. Emeleus, H. H. J.; Sharpe, A. G., *Advances in Inorganic Chemistry and Radiochemistry.* Elsevier: 1959; Vol. 1.
49. Wiberg, E., Über Den Heutigen Stand Des Borwasserstoff-Strukturproblems. *Ber. Dtsch. Chem. Ges.* **1936,** *69*, 2816-2842.
50. Hnyk, D.; Brain, P. T.; Rankin, D. W. H.; Robertson, H. E.; Greatrex, R.; Greenwood, N. N.; Kirk, M.; Buehl, M.; Schleyer, P. v. R., Molecular Structure of 2,4-Ethanotetraborane, $B_4H_8(CH_2)_2$, as Determined by Gas-Phase Electron Diffraction and Ab Initio Computations. *Inorg. Chem.* **1994,** *33*, 2572-2578.
51. Yan, Y.; Li, H.-W.; Maekawa, H.; Aoki, M.; Noritake, T.; Matsumoto, M.; Miwa, K.; Towata, S.-I.; Orimo, S.-I., Formation Process of $[B_{12}H_{12}]^{2-}$ From $[BH_4]^-$ During the Dehydrogenation Reaction of $Mg(BH_4)_2$. *Mater. Trans.* **2011,** *52*, 1443-1446.

Table of Contents.

$Mg(B_4H_{10})_2$ was identified as the rehydrogenable decomposition intermediate in the first step of $Mg(BH_4)_2$ dehydrogenation by the combined use of spectroscopic and computational methods.